PHYSICAL REVIEW E **74**, 060101(R) (2006)

Asymmetric heat conduction through a weak link

B. Hu,[1,2] D. He,[1] L. Yang,[1,3,*] and Y. Zhang[1]

[1]*Department of Physics, Centre for Nonlinear Studies, and The Beijing-Hong Kong-Singapore Joint Centre for Nonlinear and Complex Systems (Hong Kong), Hong Kong Baptist University, Kowloon Tong, Hong Kong, China*

[2]*Department of Physics, University of Houston, Houston, Texas 77204-5005, USA*

[3]*Institute of Modern Physics, Chinese Academy of Science, Lanzhou, China and Department of Physics, Lanzhou University, Lanzhou, China*

(Received 8 October 2005; revised manuscript received 17 August 2006; published 4 December 2006)

We study the heat conduction of two nonlinear lattices joined by a weak harmonic link. When the system reaches a steady state, the heat conduction of the system is decided by the tunneling heat flow through the weak link. We present an analytical analysis by the combination of the self-consistent phonon theory and the heat tunneling transport formalism, and then the tunneling heat flow can be obtained. Moreover, the nonequilibrium molecular dynamics simulations are performed and the simulations results are consistent with the analytical predictions.

DOI: 10.1103/PhysRevE.74.060101 PACS number(s): 05.70.Ln, 44.10.+i, 05.60.−k

The study of electric currents has led to the invention of electric rectifiers, diodes, and transistors. An interesting problem is the following: Can we design a thermal diode as we do for electric conductivity? A thermal diode refers that its heat fluxes will be different, as it is inversed between two heat baths. The absolute values of two different total heat fluxes are marked as $|J_{\pm}|(|J_{+}|>|J_{-}|)$; the gain of a thermal diode is defined as $r=|J_{+}|/|J_{-}|$. Very recently, Terraneo, Peyrard, and Casati [1] pointed out the possibility of the design of a thermal diode by coupling three nonlinear chains, where a strongly Morse on-site potential lattice is sandwiched between two weakly Morse on-site potential lattices. Li, Wang, and Casati [2] addressed a higher-gain model that consists of two coupling Frenkel-Kontorova (FK) lattices connected by a harmonic spring. Hu and Yang [3] try to use two FK lattices of different periodic on-site potential to design a more effective thermal diode. Other possibilities [4,5] to design a thermal diode are discussed too.

When the temperature of a nonlinear lattice changes, the effective phonon band of the lattice can shift due to the nonlinear effect. For the models of the thermal diode [1–3], the phonon bands of different segments change from the overlap status to the separation status, as right and left heat baths exchange their temperature. The nonequilibrium molecular dynamics (NEMD) simulations show that the models work well on some parameters. However, there are puzzles in the NEMD simulations results [2,3,5]. For example, why will the gain of the thermal diodes r decrease by the system size N? Why is $|J_{\pm}|$ in direct proportion to k_3^2 as $k_3\rightarrow 0$? Why does $|J_{\pm}|$ of the models coupled by two FK lattices increase by the system size N, while each FK lattice obeys the Fourier law and its total heat flux is independent of the system size N? Particularly, the exact method to estimate the behaviors of the models is still absent. So, we present an analytical method to quantitatively characterize the thermal diode based on the shift of the effective phonon band. Furthermore, we compare the analytical results to the NEMD simulations results.

In this paper, we consider a model of the thermal diode that consists of two different Morse on-site potential lattices coupled by a weak harmonic spring. Two heat baths respectively connect to two ends of the model. The two lattices will achieve two nearly equilibrium states of different temperatures, since the strength of the harmonic spring is weak. Then the self-consistent phonon (SCP) theory can take into consideration the nonlinearity of the lattices. The SCP theory has been applied to deal with the nonlinear Morse on-site potential for the DNA denaturation problem [6]. Thus we can use the general thermal tunneling transport formalism [7] to calculate the heat flux through the weak harmonic spring. When the system approaches the steady state, the heat flux in every site should be identical and the total heat flux can be obtained.

The Hamiltonian is

$$H = H_L + \frac{k_3}{2}(q_1 - q_0)^2 + H_R,$$

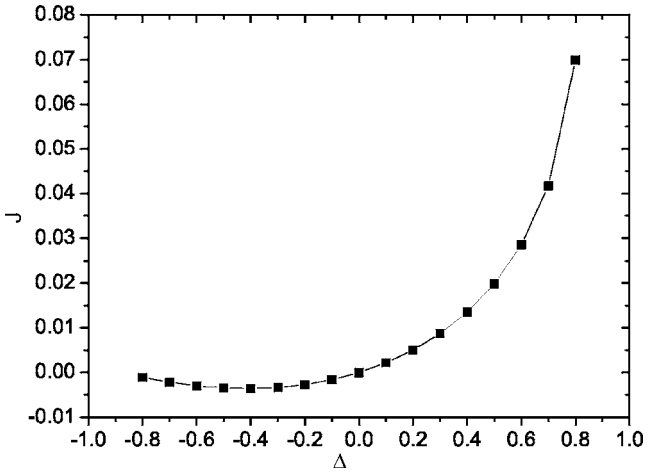

FIG. 1. Plot of J versus the dimensionless temperature difference Δ at $T_0=13.33$. $k_3=0.05$. Here J is obtained on the thermodynamical limit and $k_3\rightarrow 0$.

*Corresponding author.

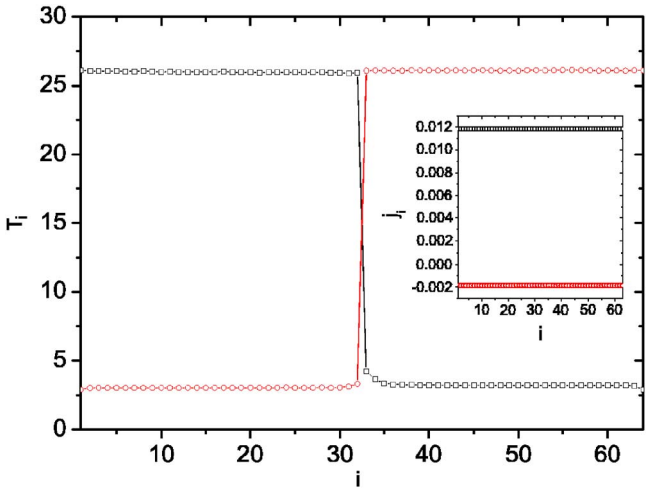

FIG. 2. (Color online) Plot of temperature profiles T_i; the inset shows the heat flux. Here, $N=64$, $T_+=26$, and $T_-=3$.

$$H_L = \sum_{i=-N/2+1}^{0} \left(\frac{p_i^2}{2m_i} + \frac{k_1}{2}(q_{i+1}-q_i)^2 + D_1(e^{-\alpha_1 q_i}-1)^2 \right),$$

$$H_R = \sum_{i=1}^{N/2} \left(\frac{p_i^2}{2m_i} + \frac{k_2}{2}(q_{i+1}-q_i)^2 + D_2(e^{-\alpha_2 q_i}-1)^2 \right), \quad (1)$$

where N is the total number of the particles, $m_i=1$ the mass of particles, p_i the momentum of the ith particle, and q_i its displacement from the equilibrium position. k_1, k_2, and k_3 are the strength of the interparticle harmonic potential, $k_1=k_2=1$. For the left segment $D_1=30$, and $\alpha_1=0.316$; for the right segment $D_2=20$ and $\alpha_2=0.316$. When the heat bath T_+ connects with the ith $(i=-N/2+1)$ particle, T_- connects with the ith $(i=N/2)$ particle, the heat flux j_+ goes through the system, and $J_+=j_+N$ is the total heat flux. When the heat bath T_- connects with the ith $(i=-N/2+1)$ particle, T_+ connects with the ith $(i=N/2)$ particle, the heat flux j_- goes through the system, and $J_-=j_-N$ is the total heat flux.

H_L and H_R can be approximated [6] by the SCP theory as

$$H_L' = \sum_{i=-N/2+1}^{0} \left(\frac{p_i^2}{2} + \frac{k_1}{2}(q_{i+1}-q_i)^2 + \frac{f_1}{2}q_i^2 \right),$$

$$H_R' = \sum_{i=1}^{N/2} \left(\frac{p_i^2}{2} + \frac{k_2}{2}(q_{i+1}-q_i)^2 + \frac{f_2}{2}q_i^2 \right), \quad (2)$$

where the effective harmonic potential coefficient $f_l(T)$ $(l=1,2)$ is obtained from the self-consistent equation $\ln(2\alpha_l^2 D_l/f_l)=(\alpha_l^2 k_B T/N)\Sigma_p\{1/[f_l+4k_l \sin^2(p\pi/N)]\}$.

The general heat flux formula across the weak harmonic spring is

$$J = \sum_{k>0} E_k v_k \alpha_k + \sum_{q<0} E_q v_q \alpha_q, \quad (3)$$

where E_k and E_q are the energy in the kth and qth mode, respectively, v_k and v_q the phonon group velocities on the left and right segments, and α_k and α_q the transmission coefficients. Here the reasonable mode-energy distributions of the classical system take $E=k_BT$. The effective phonon group velocities can be obtained from the effective Hamiltonian (2). For the transmission coefficients, we assume a wave incident from the left, which is reflected by the interface with amplitude r and transmits across the interface with amplitude t on the right:

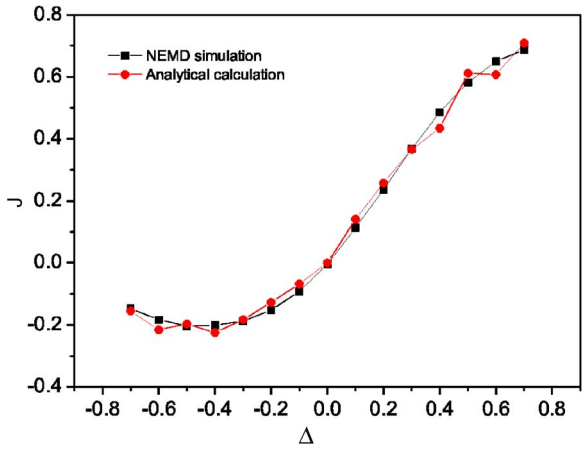

FIG. 3. (Color online) Plot of J versus the dimensionless temperature difference Δ at $T_0=13.33$. Here $k_3=0.05$ and $N=64$.

$$q_i = e^{Ikia_1} + re^{-Ikia_1}, \quad i \leqslant 0,$$

$$q_i = te^{Iq(i-1)a_2}, \quad i \geqslant 1, \quad (4)$$

where I is the imaginary number unit. Through a tedious but straightforward algebraic manipulation, one obtains the transmission coefficient

$$\alpha = 2\sin(ka_1)\sin(qa_2)k_3^2 \Big/ \Big(2[\cos(ka_1)\cos(qa_2) - \cos(ka_1) - \cos(qa_2) + 1][k_1k_2 - (k_1+k_2)k_3] + 1 + \frac{k_1}{k_2} + \frac{k_2}{k_1} + \cos(ka_1 - qa_2) - \frac{k_1+k_2}{k_2}\cos(ka_1) - \frac{k_1+k_2}{k_1}\cos(qa_2)\Big). \quad (5)$$

Thus the heat flux across the weak harmonic spring is obtained.

As $k_3 \to 0$, the transmission coefficient is

$$\alpha(\omega) \approx \frac{k_3^2}{k_1k_2}\sqrt{\frac{(f_1+4k_1-\omega^2)(f_2+4k_2-\omega^2)}{(\omega^2-k_1)(\omega^2-k_2)}}, \quad (6)$$

where $\omega^2=f_1+4k_1\sin^2(ka_1/2)=f_2+4k_2\sin^2(ga_2/2)$. In the thermodynamical limit, we can use the integral by ω substituting the sum by q in formula (3),

$$J = k_B(T_+ - T_-)\int_{\omega_{\min}}^{\omega_{\max}} \alpha(\omega)d\omega. \quad (7)$$

Bringing the formula (6) into the formula (7), we obtain

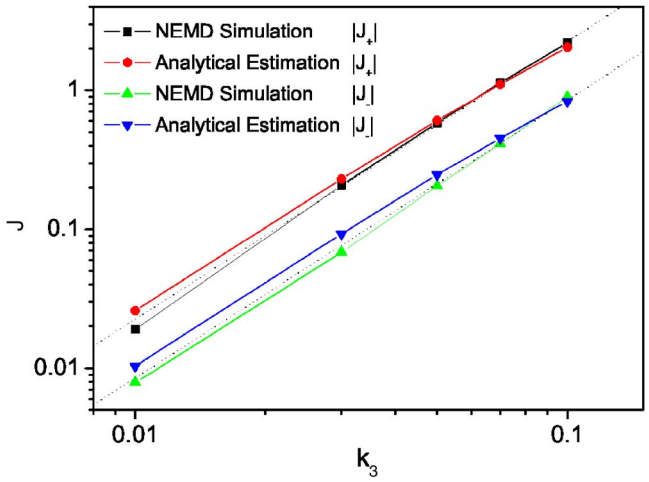

FIG. 4. (Color online) Plot of J versus k_3. Here $T_0=13.33$ and $\Delta=0.5$.

$$j_+ = \frac{k_B(T_+ - T_-)k_3^2}{k_1 k_2} \times \int \sqrt{\frac{[f_1(T_+) + 4k_1 - \omega^2][f_2(T_-) + 4k_2 - \omega^2]}{[\omega^2 - f_1(T_+)][\omega^2 - f_2(T_-)]}} d\omega,$$

$$j_- = -\frac{k_B(T_+ - T_-)k_3^2}{k_1 k_2} \times \int \sqrt{\frac{[f_1(T_-) + 4k_1 - \omega^2][f_2(T_+) + 4k_2 - \omega^2]}{[\omega^2 - f_1(T_-)][\omega^2 - f_2(T_+)]}} d\omega, \quad (8)$$

where f_l satisfied $\ln(2\alpha_l^2 D_l/f_l)=\alpha_l^2 k_B T/\sqrt{f_l^2+4k_l f_l}$ $(l=1,2)$. Then one can obtain the relation of the strength of the weak harmonic spring and the heat flux, $J_\pm \sim k_3^2$. In Fig. 1, the relation between the total heat flux J (J_+ and J_-) and Δ is shown, where Δ is defined as $T_\pm=T_0(1\pm\Delta)$. J increases as Δ for $\Delta>0$ and J is nearly zero for $\Delta<0$. As $\Delta<-0.9$, J is exactly equal to zero and the gain $r\to\infty$. The results are qualitatively the same as the NEMD simulations results of a similar model in Refs. [2,5].

The NEMD simulations are performed on the model. The heat baths are implemented as Nose-Hoover [8] baths in the simulations. The particles from $i=-N/2+2$ to $i=N/2-1$ follow the Hamiltonian equations of motion, while $\ddot{q}_{-N/2+1}=-\xi_\pm \dot{q}_{-N/2+1}-\partial H/\partial q_{-N/2+1}$, $\ddot{q}_{N/2}=-\xi_\mp \dot{q}_{N/2}-\partial H/\partial q_{N/2}$, and $\xi_\pm=\dot{q}_{-N/2+1}^2/T_\pm-1$, $\xi_\mp=\dot{q}_{N/2}^2/T_\mp-1$. The heat flux j takes the general expression of the heat flux [9]. Richardson's method is used on the integration [10]. The total integration time is typically $\cong 10^8-10^9$ units.

Figure 2 shows typical temperature profiles of the system and the inset shows the heat flux profiles at the same parameters, in this case $|J_+|>|J_-|$ and $r\sim 6$. The left and right segments achieve nearly two equilibrium states on two heat baths' temperature, respectively. For the NEMD simulations results in Fig. 3, Fig. 4, and Fig. 6, the temperature profiles are checked to ensure nearly equilibrium states.

The relation of J and Δ is shown in Fig. 3; the line indicates only the line of sight. Here the solid circles show J by the analytical estimations with formula (3) at finite size $N=64$. The solid squares show J by the NEMD simulations. The two curves exhibit similar behaviors; the difference between two sets of data is generally less than 10%. They both show a clear rectifying effect. We also investigate the relation of $|J_\pm|$ and k_3 in Fig. 4. The NEMD simulations are consistent with the analytical estimations, and they both show the relation $|J_\pm|\sim k_3^2$ as $k_3<0.1$; the dotted lines show the functions $|J_\pm|\propto k_3^2$. The results show well the consistency of the NEMD simulations and the analytical estimations.

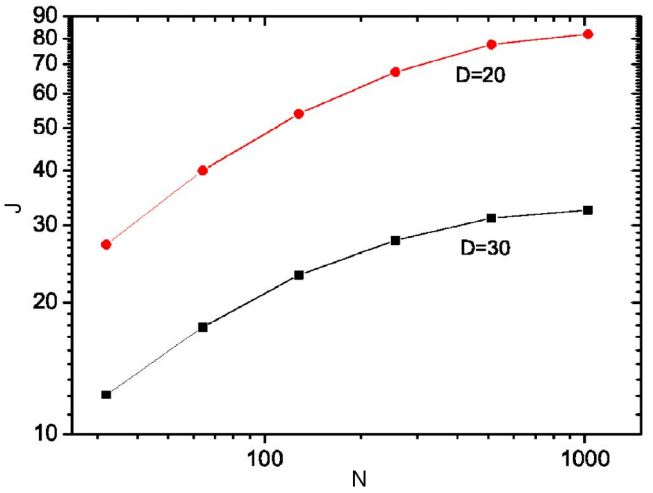

FIG. 5. (Color online) Plot of J versus N for pure Morse on-site potential models H_L $(D=30)$ and H_R $(D=20)$.

For the nonlinear on-site potential lattice, its thermal conductivity obeys Fourier's law and its total heat flux is independent of the system size. However, the simulation results show that the total heat flux of the two segment diode models [2,3] increase by the system size N, where each segment is a FK lattice. For the model (1), the dependence of J to N for each segment is shown in Fig. 5. As the system size changes from $N=128$ to 1024, the total heat fluxes J of H_L or H_R approach a constant as expected. In Fig. 6, the dotted lines show the functions $|J_\pm|\propto N$; for the model (1) the NEMD simulation results and the analytical estimations of the total

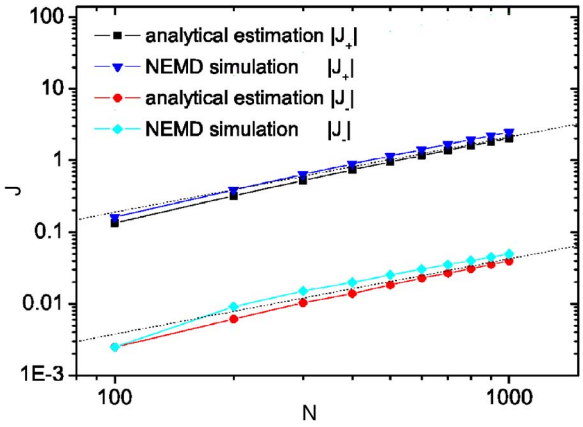

FIG. 6. (Color online) Plot of J versus N; here $T_0=13.33$, $\Delta=0.5$, and $k_3=0.05$.

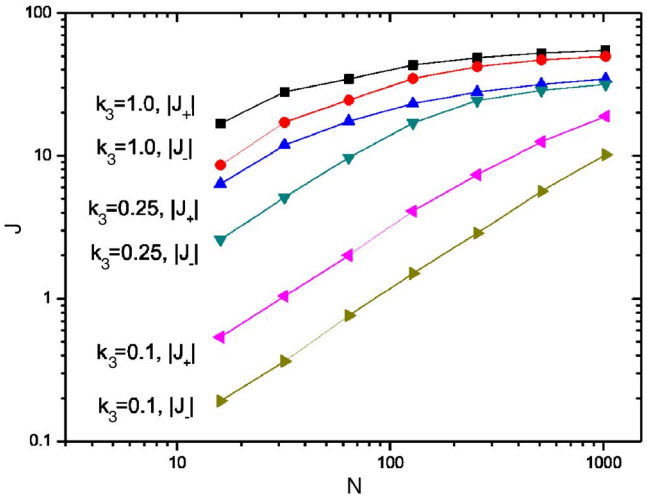

FIG. 7. (Color online) Plot of J versus N; here $T_0=13.33$ and $\Delta=0.5$.

heat flux $J(N)$ are shown. They nearly overlap and $|J_{\pm}|$ is in direct ratio to the system size N.

Here we need to clarify that the analytical estimation holds true only as the coupling between two segments is weak enough. Figure 7 shows the NEMD simulation results for different k_3 as the system size N increases. For $k_3=0.25$, the NEMD simulation results leave the analytical estimations ($|J_{\pm}| \propto N$) at the separate point $N_0 \approx 100$. For $k_3=0.1$, the separate point N_0 is larger than 1000. The separate point N_0 increases as k_3 decreases. This means that the NEMD simulations will separate from the analytical estimations as the coupling k_3 is strong enough for a fixed system size N. When we check the temperature profiles, the two segments are no longer nearly in equilibrium states. The analytical analysis is not reliable on these cases.

In summary, we consider a model consisting of two different Morse on-site potential lattices coupled by a weak harmonic spring. Using the SCP theory and the general thermal tunneling transport formalism, the heat flux through the system can be estimated. The NEMD simulations are also performed. As k_3 is small enough for a fixed N, one can predict the NEMD simulation results by the analytical estimations quite well.

We would like to thank members of the Centre for Nonlinear Studies for useful discussions. L.Y. acknowledges the support of the 100 Person Project of the Chinese Academy of Sciences. This work was supported in part by grants from the Hong Kong Research Grants Council (RGC) and the Hong Kong Baptist University Faculty Research Grant (FRG).

[1] M. Terraneo, M. Peyrard, and G. Casati, Phys. Rev. Lett. **88**, 094302 (2002).
[2] B. Li, L. Wang, and G. Casati, Phys. Rev. Lett. **93**, 184301 (2004).
[3] B. Hu and L. Yang, Chaos **15**, 015119 (2005).
[4] D. Segal and A. Nitzan, Phys. Rev. Lett. **94**, 034301 (2005); B. Xie, H. Li, and B. Hu, Europhys. Lett. **69**, 358 (2005).
[5] B. Hu, L. Yang, and Y. Zhang, Phys. Rev. Lett. **97**, 124302 (2006); B. Hu, L. Yang, and Y. Zhang, report of CNS0504, 2005 (unpublished).
[6] T. Dauxois, M. Peyrard, and A. R. Bishop, Phys. Rev. E **47**, 684 (1993).
[7] G. P. Srivastava, *The Physics of Phonons* (IOP Publishing Ltd, Bristol, 1990).
[8] S. Lepri, R. Livi, and A. Politi, Phys. Rep. **377**, 1 (2003).
[9] R. Kubo, M. Toda, and N. Hashitsume, *Statistical Physics II*, Springer Series in Solid State Sciences Vol. 31 (Springer, Berlin, 1991).
[10] J. Stoer and R. Bulirsch, *Introduction to Numerical Analysis* (Springer-Verlag, New York, 1980), Chap. 7, Sec. 2.14.